Fingerprint Matching Using Minutia Polygons

Xuefeng Liang, Tetsuo Asano
Japan Advanced Institute of Science and Technology
JAIST, 1-1, Asahidai, Nomi, Ishikawa 923-1292 Japan
{xliang, t-asano}@jaist.ac.jp

Arijit Bishnu
Indian Institute of Technology
Kharagpur 721302, India
Arijit.Bishnu@iitkgp.ac.in

Abstract

Fingerprint distortion changes both the geometric position and orientation of minutiae, and leads to difficulties in establishing a match among multiple impressions acquired from the same finger. In this paper, minutia polygons are used to match distorted fingerprints. A minutia polygon describes not only the minutia type and orientation but also the minutia shape. This allows the minutia polygon to be bigger than the conventional tolerance box without losing matching accuracy. In other words, a minutia polygon has a higher ability to tolerate distortion. Furthermore, the proposed matching method employs an improved distortion model using a Multi-quadric basis function with parameters. Adjustable parameters make this model more suitable for fingerprint distortion. Experimental results show the proposed method is two times faster and more accurate (especially, on fingerprints with heavy distortion) than the method in [1].

1. Introduction

One of the main difficulties in matching two impressions of the same finger is dealing with non-linear *distortions*. Distortion arises from the elasticity of finger skin, the pressure, and the movement of fingers during image capture. It changes the mutual spatial locations of minutiae, which leads to great difficulties in establishing a match among multiple images acquired from a single finger. This paper deals with compensating for elastic distortion to improve the performance of minutiae matching.

There have been several attempts to account for the elastic distortions in fingerprint images. Senior et al. [3] proposed a canonical model which normalizes a fingerprint image to a canonical form in which all the ridges are equally spaced. This model can actually correct traction deformation very well, but torsion deformation cannot be adequately corrected. Cappelli et al. [5] proposed a distortion model which defines three distinct distortion regions according to different pressures. Experiments showed that this model provides an accurate description of the elastic distortion. However, the parameters of this model should be given by experiments, not automatically. Kovács-Vajna [7] used a triangular matching algorithm to compare two sets of minutiae and to account for elastic distortion. Ross et al. [2] attempted to build an average deformation model from multiple impressions of the same finger using a thin-plate spline (TPS) model. Since we cannot guarantee that any given pre-captured impression contains all kinds of distortions, this average deformation model does not have sufficient competence for matching. Bazen et al. [1] also used a TPS model to align all possible matched pair of impressions. Owing to iteratively aligning minutiae between input and template impressions, a risk of forcing an alignment between impressions originating from two different fingers arises, and leads to a higher false accept rate.

Normally, minutiae matching has two stages: 1. Registration aligns fingerprints, which could be matched, as well as possible; 2. Evaluation calculates matching scores using a tolerance box between every possibly matched impression pairs. In this paper, *minutia polygons* are incorporated in both the registration and evaluation stages. As minutia shapes are included, the proposed method provides more accurate matching results. We also improved the distortion model as in [1] by using a Multi-quadric function instead of TPS, since the Multi-quadric function has higher capability for interpolating scatter minutiae. Experiments demonstrate that using minutia polygons and a Multi-quadric function leads to a better performance compared to [1].

The rest of the paper is organized as follows. Section 2 describes the definition of minutia polygons. Section 3 gives out a matching method using minutia polygons and an improved distortion model. Experimental results are presented in Section 4. Finally, we conclude in Section 5.

2. Minutiae polygons

2.1. Polygons of bifurcation minutiae

Let p be a bifurcation minutia with three ridges incident upon it, namely, where r is the ridge before bifurcation, r_1

and r_2 are the two ridges after bifurcation. For each of r, r_1 and r_2, consider a line segment, which has length λ and is tangent to the corresponding ridge at p. Let these three line segments be $\overline{b_1p}, \overline{b_2p}$ and $\overline{ap}$ corresponding to r_1, r_2 and r, respectively (see Fig. 1). Let θ be the angle made by $\overline{ap}$, measured in counterclockwise direction with regard to x-axis. We call the group of the three line segments $\overline{b_2p}, \overline{b_1p}$ and $\overline{ap}$ as the *bifurcation detail* $\mathcal{B}(p, a, b_1, b_2)$ for minutia p.

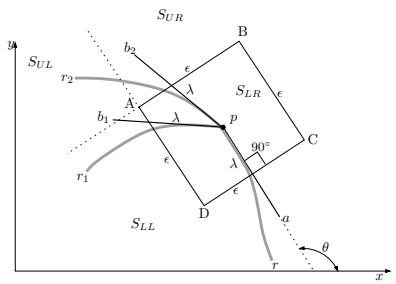

Figure 1. Minutia detail and defining ϵ-square box with regard to a bifurcation minutia at p.

Now consider a square $ABCD = \mathcal{S}(p, \theta, \epsilon)$ having side length ϵ, centered about the minutia p, and having one of its sides perpendicular to $\overline{ap}$, as shown in Fig. 1. As we go on sliding the minutia p with its three line segments within the ϵ-square, we get a bifurcation polygon $\mathcal{M}$ (see Fig. 2(a)).

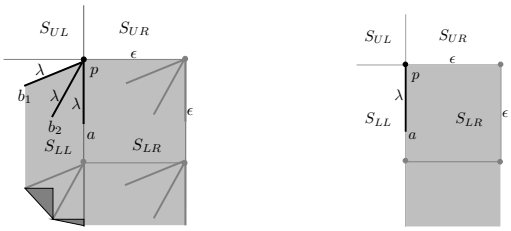

(a) Bifurcation polygon (case 1). (b) Termination polygon.

Figure 2. Minutia polygons.

The polygon $\mathcal{M}$ can have different shapes, depending on the mutual orientations of $\overline{b_1p}, \overline{b_2p}$ and $\overline{ap}$. When p coincides with A, the region around p can be divided into 4 quadrants, which are named as S_{LL} (lower left region), S_{UL} (upper left region), S_{UR} (upper right region), and S_{LR} (lower right region), as shown in Fig.2(a). Each of b_1 and b_2 can lie in any one of these 4 regions, thereby making $4 \times 4 = 16$ possibilities. Out of these 16 possibilities, however, there will be 10 cases having distinct mutual positions of b_1 and b_2, considering the inter-changeability of b_1 and b_2. That is, for example, the case of $b_1 \in S_{LR}$ and $b_2 \in S_{UR}$, and the case of $b_2 \in S_{LR}$ and $b_1 \in R_{UR}$, which are 2 different cases in 16 possibilities, are the same in the later 10 cases. These 10 cases are enumerated in Fig.3. Cases 2, 6 and 9 can have two subcases each, depending on the relative x-axis (or, y-axis) coordinates of b_1 and b_2, which will have differently shaped polygons of $\mathcal{M}$. Hence we get $7 + 6 = 13$ different polygons (See Fig.2(a) and 3).

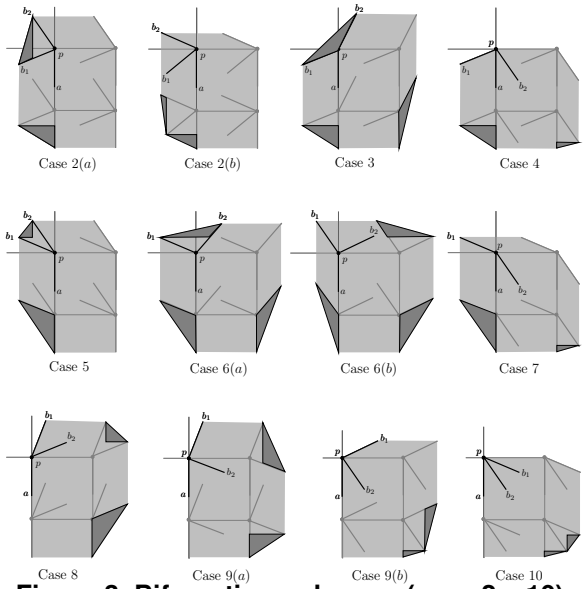

Figure 3. Bifurcation polygons (case 2 – 10).

For a valid bifurcation minutia p, the angle $\angle(b_1, p, b_2)$ should be less than both $\angle(b_1, p, a)$ and $\angle(b_2, p, a)$, which helps us to distinguish r from r_1 and r_2. Keeping this point in consideration, out of the above 13 cases, cases 3, 4 and 7 are not possible for a valid bifurcation minutia. Hence we have only $13-3 = 10$ possible differently shaped polygons.

2.2. Polygon of termination minutiae

Let p also be a termination minutia. As there is only one ridge r incident upon it, termination detail $\mathcal{T}(p, a)$ has just one line segment $\overline{ap}$ corresponding to r, which is defined similar to bifurcation detail. So, only the line segment $\overline{ap}$ contributes to termination polygon. Analogously sliding the minutia p with line segment $\overline{ap}$ within square $\mathcal{S}(p, \theta, \epsilon)$, we get a termination polygon $\mathcal{M}$, i.e. a rectangle (see Fig. 2(b)). Certainly, the shape of termination polygon is unique.

3. Minutiae matching

To identify a input fingerprint with distortion among templates stored in a database, our algorithm contains three stages: first of all, pick out those possibly matched templates according to local similarity measures (Section 3.1). Next, estimate a global non-rigid transformation between each possibly matched pair (Section 3.2). Finally, calculate and evaluate the matching scores (Section 3.3).

3.1 Alignment of minutiae set

To find possibly matched templates, our matching algorithm relies on correct correspondences of minutiae patterns. This step greatly affects the efficacy and efficiency

of distortion estimation. The basic idea of our approach is based on the observation that, even if an elastic distortion is applied to a fingerprint image, every minutia always keeps the same neighbor structure. We use this idea, employing minutia polygons and invariants of each minutia with respect to its neighbors. Some similar methods have been proposed in the literature. Jiang et al. [6] proposed a matching approach using local structure represented by a minutia and its two nearest neighbors. In [1], this idea was slightly modified to improve reliability. However, their time complexity is $O(n^2)$ at least. Parziale et al. [4] used minutiae triangulation to describe the local structure and decreased the time complexity to $O(n \log n)$. Since these triangles include less information about minutiae, more factors must be considered to achieve satisfied matching result.

As a simple and explicit definition of minutia polygon, and uniqueness and reliability of Delaunay triangulation, we incorporate them in alignment step. Let $\mathcal{M}^I_{p_i,\theta_i}(i = 1 \ldots n)$ denote the polygon case with position and orientation of the ith minutia in an input fingerprint. In a template fingerprint, we have similar polygon case $\mathcal{M}^T_{p_j,\theta_j}(j = 1 \ldots m)$. Once the minutiae have been extracted, their Delaunay triangulation can be obtained. Here, each Delaunay triangle and its edges are reliable descriptions of local structure. Therefore, we compute invariants related to the positions and angles of the minutiae for each triangle edge:

$$(L,\ \phi_1,\ \phi_2,\ \mathcal{M}_1,\ \mathcal{M}_2)$$

where L is the length of triangle edge; ϕ_1 and ϕ_2 are the angles between the edge and line segments $\overline{ap}$ at two end points respectively; $\mathcal{M}_1$, $\mathcal{M}_2$ are minutia polygon cases of two end points.

To compare two edges in input and template fingerprints, $(L,\ \phi_1,\ \phi_2,\ \mathcal{M}_1,\ \mathcal{M}_2)$ values are used, all of which are invariant of the translation and rotation. We assume two edges match if they satisfy the following set of conditions:

$$\frac{|L^I - L^T|}{max(L^I, L^T)} < t_1$$

$$|\phi_1^I - \phi_1^t| < t_2;\ \ |\phi_2^I - \phi_2^t| < t_2$$

$$\mathcal{M}_1^I = \mathcal{M}_1^T;\ \ \mathcal{M}_2^I = \mathcal{M}_2^T$$

where t_i is a threshold, and its value is dependent on images.

If one edge from an input image matches two or more edges in a template image, we need to consider the triangle to which this edge belongs and compare the triangle pair. With the same strategy, our method retrieves five template fingerprints, which have the most matched triangle edges, from database. Each of these matched edges represents a hypothetical correspondence between minutiae in the input and template fingerprints. These correspondences are the control-points we expect for our estimation of a elastic distortion model.

3.2. Estimation of elastic distortion

The next step is to estimate the global non-rigid transformation that can register two fingerprints for final matching. Referring to the obtained local correspondences from alignment step, the global non-rigid transformation is estimated. This transformation is expected to explicitly map the input fingerprint to a template one with aim of obtaining the largest amount of matched minutiae pairs.

With control-points, the estimation of elastic distortion can be treated as a scattered data interpolation problem. One way of approaching interpolation is to use *Radial Basis Function* (RBF). RBF offers several advantages: first of all, the geometry of the control-points is by no means restricted; secondly, the RBF provides easily controllable behavior that can be tailored to meet specific requirements. An RBF may be purely deformable, or it may contain some form of linear component, allowing both local and global deformations. Bazen et al. [1] first proposed a Thin-plate spline model for elastic distortion and reported a good result. Essentially, Thin-plate spline (TPS) is one of the RBF basis functions. The choice of a basis function is determined by the interpolation conditions and the desired properties of the interpolation. Since fingerprint distortion is elastic rather than viscous/rigid, the influence of control-points on the distorted fingerprint increases with distance at a certain range from the center. On the other hand, fingerprint distortion is not globally uniform. For instance, if one side of a traction deformation center is compressed, the opposite side must be dilated. Both the TPS ($r_i^2 \log r_i$) and Multi-quadric ($(r_i^2 + \delta)^{+\mu}$) basis functions monotonically increase with distance from the center, where r_i is the distance between control-points. However, the Multi-quadric basis function (MQ) has another advantage: parameters (locality parameter δ and exponent μ). MQ, therefore, can be tailored to many specific needs, and their range of influence can be controlled by adjusting the parameters. As the property of fingerprint distortion, we would like to control the area of influence of basis function. *Locality parameters*, which can control the range of influence of a basis function, can perform this task. They give less weight to distant control-points and more weight to neighboring ones. A locality parameter uses unique values δ_i for each control-point, calculated from the distance to the nearest neighboring control-point. This essentially allows the distortion to be softer where control-points are widely spaced and stronger where they are closer together, which may work more effectively on fingerprint minutiae. Using this adaptive locality parameter, MQ is modified as: $g(r_i) = (r_i^2 + \delta_i)^{\mu}$. where $\delta_i = min_{i \neq j}(r_{ij})\ \ (j = 1, \ldots, n)$.

3.3. Final minutiae matching

Most conventional matching methods use a small circle as a tolerance box. If two similar minutiae fall into the

same tolerance box, they are defined as matched. When the circle is smaller, the accuracy of identification is higher. In our work, we replace the small circle by minutia polygons. Since the minutia polygon contains more information (minutia shape), it can be bigger than a traditional tolerance box without losing accuracy. Therefore, a bigger minutia polygon has a higher ability to tolerate distortion. Our minutia matching condition is: if two minutia polygons intersect with the same case and a similar orientation, they are defined as matched. Finally, the matching score S is calculated by

$$\mathsf{S} = \frac{n_{match}^2}{n_1 n_2}$$

where n_{match} is the number of matched minutiae, n_1 and n_2 are the number of minutiae in the input and template fingerprints, respectively.

4. Experimental results

We evaluated our method by testing it on Database FVC2000 which consists of 880 fingerprints, 8 prints each of 110 distinct fingers. In addition, we also scanned 80 fingerprints with heavy distortion from a FUJITSU Fingerprint Sensor (model: FS-210u), 4 prints each of 20 distinct fingers.

Due to the lack of a benchmark of minutiae matching performance, we compared our matching method with the TPS-based algorithm in [1] on two aspects: computing time and accuracy of identification. In our method, $\epsilon = 3$ and $\lambda = 5$ were used to generate minutia polygons; $\mu = 0.2$ was employed for the MQ basis function. For TPS-based algorithm, a tolerance box with radius $r = 5$ was used. Since TPS-based algorithm uses three local structures for each minutia in the alignment step, and iteratively registers minutiae between two fingerprints, they are time consuming and lead to a higher risk of matching two similar fingerprints coming from distinct fingers. On the contrary, our method uses minutiae polygons and triangle edges for alignment, so there are fewer comparisons. Moreover, parameters tailor the MQ basis function more suitable for elastic distortion, and minutia polygon works as a tolerance box with a higher ability to tolerate distortion. With these two advantages, our matching does not need iteration for registering minutiae. Therefore, our method, in practice, is around two times faster than TPS-based algorithm on average. Matching performance (ROC) curves plotting the false reject rate (FRR) against the false accept rate (FAR) at various thresholds are presented in Fig. 4. For the data in FVC2000, two methods have almost same accuracy, but for the scanned fingerprints with heavy distortion, our method is more accurate. We believe that this is due to minutia polygon has a higher ability to tolerate distortion and the MQ basis function can be tailored by parameters for this particular problem. To sum up, our matching method using minutia polygons not only provides computational efficiency, but also leads to better performance in matching.

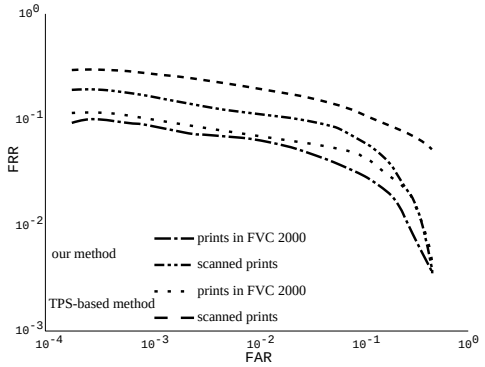

Figure 4. ROC curves on FVC2000 DB and scanned fingerprints obtained with the proposed method and the algorithm in [1].

5. Conclusions

We have proposed a matching method using minutia polygons. A minutia polygon describes not only the minutia type and orientation but also the minutia shape. This allows minutia polygon to be bigger than the conventional tolerance box without losing matching accuracy. In other words, minutia polygon has a higher ability to tolerate distortion. Our method also improves the distortion model in [1] using MQ basis function with parameters. Adjustable parameters make the improved model more suitable for fingerprint elastic distortion than the TPS-based model. Our future efforts will target a more in-depth study of the properties of minutia polygon that can be used in distorted fingerprint matching.

References

[1] A.M.Bazen and S.H.Gerez. Fingerprint matching by thin-plate spline modelling of elastic defromations. *Pattern Recognition*, 36(8):1859–1867, 2003.

[2] A.Ross, S.C.Dass, and A.K.Jain. A deformable model for fingerprint matching. *Pattern Recognition*, 38(1):95–103, 2005.

[3] A.Senior and R.Bolle. Improved fingerprint matching by distortion removal. *IEICE Trans.INF. & SYST.*, E84-D(7):825–832, 2001.

[4] G. Parziale and A. Niel. A fingerprint matching using minutiae triangulation. *Proc. of ICBA*, pages 241–248, 2004.

[5] R.Cappelli, D.Maio, and D.Maltoni. Modelling plastic distortion in fingerprint images. *Proc. of CAPR*, 1:369–376, 2001.

[6] X.Jiang and W.Y.Yau. Fingerprint minutiae matching based on the local and global structures. *Proc. of ICPR*, 2:1042–1045, 2000.

[7] Z.M.Kovács-Vajna. A fingerprint verification system based on triangular matching and dynamic time warping. *IEEE Trans. on PAMI*, 22(11):1266–1276, 2000.